

## Improve leakage management to reach sustainable water supply networks through by green energy systems. Optimized case study

Carlos Andrés Macías Ávila <sup>a</sup>, Francisco-Javier Sánchez-Romero <sup>b</sup>, P. Amparo López-Jiménez <sup>a</sup>, Modesto Pérez-Sánchez <sup>a,\*</sup>

<sup>a</sup> Hydraulic and Environmental Engineering Department, Universitat Politècnica de València, Valencia 46022, Spain

<sup>b</sup> Rural and Agri-food Engineering Department, Universitat Politècnica de València, Valencia 46022, Spain



### ARTICLE INFO

#### Keywords:

Leakages  
Sustainable water supply system  
Green water management

### ABSTRACT

The cities and townships should increase their sustainability to achieve the different targets, which are included in the sustainable development goals. The water distribution networks are present in urban areas. It implies the improvement of their management is key to reaching this sustainability. The water managers use different strategies to reach sustainable values in their facilities, searching for the reduction of the leakage volume. The proposed research develops a new methodology, which enables the self-calibration of leaks in water supply, knowing the injected flow and the consumed volume in the water networks. Besides, the proposed tool enabled the incorporation of the recovery systems to improve the energy efficiency of the network, increasing the use of renewable energies and reducing the leakages volume. These improvements affect positively the hydraulic efficiency of the system, and therefore, it improves the use of the water resources of the cities and reduces the cost for the citizens. The methodology was applied to a real case study located in Manta (Ecuador). The proposed procedure, which is optimized by two simulated annealing procedures inserted in an iterative procedure enables the decreased volume of the leakages above 120000 m<sup>3</sup> and increased the annual generated renewable energy by 34490 kWh, decreasing the emission of 969 tCO<sub>2</sub> each year.

### 1. Introduction

Sustainability is key in the development of the improvement of the cities management, guaranteeing the supply and reducing the non-renewable resources (Jing Niu and Kai Feng, 2021). The use of new technologies to reduce the leakages volume is crucial since this lost volume is considerably high around the world. Its control is essential to meet the increasing water demand caused by rapid population growth and urbanization (Islam and Babel, 2013) towards smart water management cities (Bibri and Krogstie, 2017). Currently, water leaks in water networks are a worldwide problem. Water losses vary between 8 and 24% in developed countries. These values oscillate between 15 and 24% in recently industrialized countries and they are between 25 and 45% in developed ones (Farley, 2001). In the United States and the United Kingdom, the leakages range is between 10% and 30% (Beuken et al., 2007). As another example, the lost volume by leakages is 37% in South Africa (Lambert, 2002), estimating the cost/value of water lost amounts to USD 39 billion per year (Liemberger and Wyatt, 2019).

The leakages estimations could be developed by different methods applied in water distribution networks by operation strategies for their detection (Li et al., 2015). One of them is Torricelli's theorem (Samir et al., 2017), which is dependent on pressure, orifice area and a discharge coefficient. Another commonly used method to determine leaked volume is FAVAD (Fixed and Variable Area Discharges) equation, this indicates that the cross-sectional area of some types of leaks (holes, breaks in tubes, joints or fittings) can also vary with pressure, while the flow velocity continues to vary with the square root of pressure (Schwaller et al., 2015). This method was applied to a real case in a water distribution network in Kwadabeka, South Africa (Deyi et al., 2014). Another strategy was based on the FAVAD concept. It is the N1 Power Law (Lambert et al., 2017). It increased its use since 1994 for practical assessment of pressure-dependent leakage in water distribution systems. Explains a study on the relationship between pressure and leakage, and guides equations for data analysis and prediction in individual situations (Lambert, 2000). This method contains in its equation a leak coefficient C and the leak exponent N1 that has been evaluated in

\* Corresponding author.

E-mail address: [mopesan1@upv.es](mailto:mopesan1@upv.es) (M. Pérez-Sánchez).

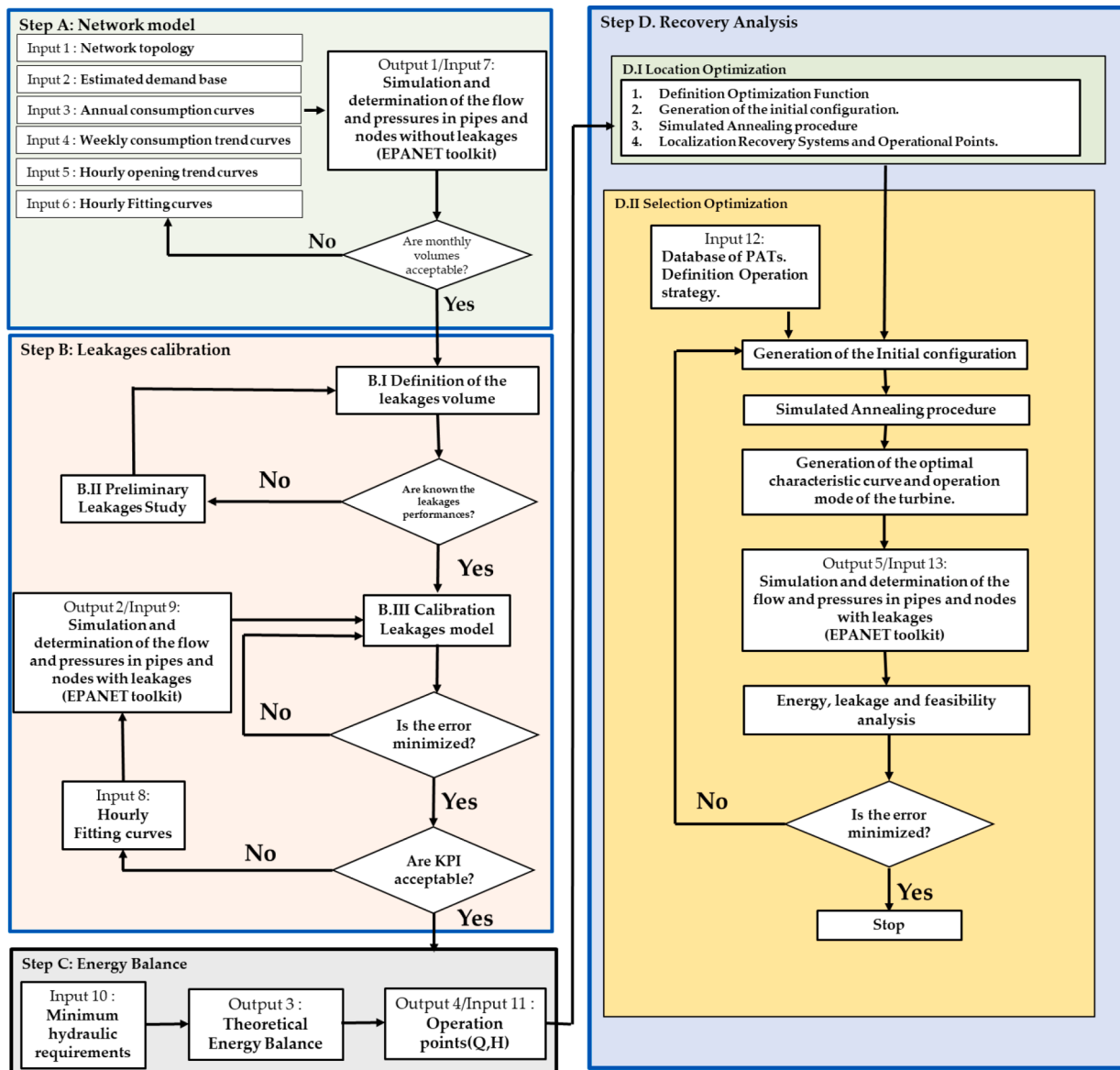


Figure 1. Proposal of the optimization procedure.

different investigations and can vary from 0.5 to 2.3 depending on the material and type of failure (Ferraiuolo et al., 2020).

The estimation of the leakage is not enough and the modelling is necessary to carry out the different simulations in the water distribution system. In this line, two different modellings were used by different authors. The minimum night flow was proposed by (Serafeim et al., 2022). This method is the most popular for estimating real leaks, under the assumption that during the last hours of the night and the first hours of the morning consumption is minimal and pressure is high. (AL-Washali et al., 2018) established a minimum night flow analysis, which was carried out on a district metered area (DMA) in an intermittent supply system in Zarqa, Jordan.

The other modelling concept was proposed by Canto Ríos et al. (2014) that showed the equations of the BABE (Burst and background estimates) method. This method enables the determination of the background losses and leaks, considering that the leaks occur along the pipe. Whatever method is used, most of the leaks can be avoided. However, there was an unavoidable part, even in new or well-managed water distribution networks (Lambert et al., 1999). In water distribution networks, leakage types have evolved into three categories namely reported, unreported, and background leakage. Reported and unreported

leakage are defined as burst or mains leakages and are caused by structural pipe failure (Adedeji et al., 2017). In this line, the researchers tried to reduce the leakages volume by management of the water distribution networks using pressure reduction valves (Schwaller and van Zyl, 2015). For example, the reduction from 39 to 31 m w.c. the daily water loss was reduced by 20.52%, respectively, and the average critical point pressure is reduced by 21.13% (Wu et al., 2013).

The leakages reduction can develop using pressure reduction valves, which cause a positive impact on the hydraulic efficiency of the system but the behaviour is negative when the energy efficiency is evaluated (Gupta et al., 2017, Ferrarese et al., 2021) investigated the possibility to use green valve systems as a new smart and self-powered control device. This study was an ahead step to improving sustainability. It was aligned with other different studies that considered the use of pumps working as a turbine (PATs) in the water distribution network, replacing pressure reduction valves to reduce the reliance on non-renewable energy. In Kozani (Greece) (Patelis et al., 2017), the implementation of PATs enabled the reduction of leaks in values between 20 and 40%. The location and selection of PATs were proposed by Lima et al. (2017), replacing the pressure reduction valves. The optimization was based on maximizing recovered energy. The volumetric efficiency increased from

0.7 to 0.9 and the annual recovered energy could be 169360 kWh. PSO algorithm was proposed to select the different PATs when the location is defined (Ebrahimi et al., 2021) reaching daily values of recovered energy equal to 182 kWh. A methodology was proposed to define scenarios and configurations for the improvement of hydraulic efficiency in water distribution systems. It was programmed on MATLAB Simulink (Rossi et al., 2019, Fecarotta and McNabola, 2017) focused on the optimal location of PATs to produce energy and reduce the leakages in water distribution networks. (Cimorelli et al., 2020) developed the optimal configuration of a chosen number of PATs, taking into account energy costs and volumes of water saved. (Nguyen et al., 2020) achieved a daily energy recovery of 1958 kWh, reducing almost half of the average excess pressure using an MINLP model. (Giudicianni et al., 2020) proposed an adaptive management framework for water distribution systems by reconfiguring the original network layout into dynamic district metered areas, improving the efficiency of the systems and showing an annual recovered energy potential of 19 MWh and leakage reduction of up to 16%. In this sustainable line, different layouts for the installation of pumps used as turbines were analyzed and compared to a couple of pressure reduction and hydropower generation in water distribution networks, showing the environmental and technical implications (Fontana et al., 2021), as well as social implications in which some authors developed a proposed mathematical algorithm (Latifi et al., 2021). It included a simulation model and optimization model based on different decision variables such as operational cost, customer satisfaction and reliability. The use of these new technologies enables the improvement of the leakage key performance indicators. It enables the evaluation of the theoretical state of the supply network through a series of criteria. (Grupo Especialista en Benchmarking y Evaluación del Desempeño de la IWA 2018). The IWA provides a series of indicators of water supply systems such as real water losses, water losses from household connections and the rate of leaks (Winarni, 2009, Ávila et al., 2021) enumerated these sustainable indicators into three different groups: energy, economic and environmental indexes.

Although different studies analyzed the improvement of the water management by PATs, this research proposes a new methodology. It is based on programming on Epanet Toolkit and the proposal enables the automatic calibration of the supply system when the consumed volume by users and the injected flow in the system are known. The methodology includes the development of the calibrated model, which is implemented by the methodology. It incorporates two simulated annealing procedures, which operate inserted in an iterative process working with discretized flows over time. This procedure allows water managers to locate the best position, choose the best machine and define the best strategy of the regulation based on different objective functions considering the leakages in the operation of the recovery system as well as its influence on the selection of the machines. As a novelty, the proposed research not only makes the model self-calibrate, but it is also able to discretize the leakage volume in the different types. The method can be applied to meshed networks considering hourly values along year.

## 2. Methodology

The proposed optimization methodology is divided into four phases. Each one is operated by different steps, inputs and conditions that the model requires to be executed are observed. As a novelty, the proposed methodology includes a self-calibration of the model to define the fit pattern consumption as well as the leakages distribution. Besides, the programming algorithm includes the operation in a meshed network.

### 2.1. Optimization stages

Fig. 1 shows the steps to carry out the optimization process, these are Network model (A), Leakages calibration (B), Energy Balance (C), and Recovery Analysis (D).

#### 2.1.1. Network model

The network model will be simulated using EPANET. The model requires six different inputs, which are: (i) Network topology (Input 1), which was obtained by the company management according to joints and pipes; (ii) Estimated demand base (Input 2). This demand was defined by the daily average flow considering the month of the maximum consumption; (iii) Annual consumption curves (Input 3) define the consumption curves, which are related to the weekly consumption trend curves (Input 4).

Input parameters are modified to define the network model. Input 2 estimated the demand base guaranteeing positive pressure in the system and there are no hydraulic scenarios, which were incoherent. Input 5 (hourly opening trend curves) and Input 6 (hourly fitting curves) were defined using the different registered volumes and flowmeters. Input 5 considers uniform average leakage flow and seeks similarity to demand-only flow estimation. Input 6 develops iterations, which adjust the fitted coefficients to the hourly fitting values. Once the model is defined, it is verified if the monthly volumes are acceptable, and it will be ready to be calibrated in the next Block B. The proposal of the model estimated the roughness according to the material and lifetime of the pipes since the case study does not install pressure sensors in the water system. The proposed methodology could incorporate a preview calibration in Step A when these data are available and it will develop an iterative procedure to minimize the error between simulated and measured pressure similar to the procedure developed in leakages calibration.

#### 2.1.2. Leakages calibration

The second step proposed for the calibration strategy considers the water leaks in the system. It is defined by considering information from the network such as the injected flow rate and consumption to establish a volume balance through the continuity equation (Step B.I). Once the leaked volume is known, the estimation of the volumetric efficiency is possible, using the following equations:

$$\eta_L = \frac{V_L}{V_I} \quad (1)$$

$$\eta_M = \frac{V_M}{V_I} \quad (2)$$

where  $\eta_L$  is the leakage performance of the water system and  $\eta_M$  is the measured volume performance of the water system;  $V_I$  is the injected volume in the network in  $m^3$ ;  $V_M$  is the total measured volume by water meters in the consumption nodes in  $m^3$ , and  $V_L$  is the total leakage volume in the water system in  $m^3$ .

If there is a lack of information to know the volume of the leak, the methodology proposes a preliminary leak analysis (Step B.II). If the leakage and volumetric ratio are known, the proposal methodology goes to Step B.III. It developed the calibration model, which distributes the leaks in different ratios.

These ratios are established according to apparent and real losses (Almandoz et al., 2005). Apparent leakages are considered in the consumption joins while the real losses are defined in the pipes. Some inherent losses, such as cleaning discharges, and hydrants, are considered apparent losses according to (Almandoz et al., 2005). The discretization of these leakages enables the definition of the following ratios:

$$\eta_{AL} = \frac{V_{AL}}{V_L} \quad (3)$$

$$\eta_{RL} = \frac{V_{RL}}{V_L} \quad (4)$$

where  $\eta_{AL}$  is the ratio between apparent and total leakages;  $V_{AL}$  is the total volume of the apparent losses in  $m^3$ ;  $\eta_{RL}$  is the ratio between real leakages and total leakages;  $V_{RL}$  is the total volume of the real losses in

$\text{m}^3$ . The apparent losses are the uncontrolled leakages in the water systems, which cannot be measured (Almando et al., 2005).

Step B.II develops a series of simulations to obtain ranges of values and to define the different scenarios correctly. As the leak volume is unknown, the methodology assigned different leak parameters in the lines. The knowledge of these ratios enables the distribution of leakages in the model. It defines the different emitter coefficients in the different iterations. To establish the criteria as a function of the leakage type, the error is analysed between simulated and measured volume. The evaluation of the leakage in lines is developed by the following expression:

$$q_{L,ij} = \beta_j L_j (\bar{P}_{ij})^N \quad (5)$$

where  $q_{L,ij}$  is the leakage flow for the line at the time  $i$ ; where  $\beta_j$  is the leakage coefficient, which characterizes the pipe in terms of age, diameter, material, thickness, among others. In Step B.II, the model does not need to iterate since the used emitter coefficient in EPANET is:

$$K_j = \beta_j L_j \quad (6)$$

$\bar{P}_{ij}$  is the average pressure in the line  $j$  at the time  $i$ ;  $L_j$  is the length of the line  $j$  in meters;  $N$  is the leakage exponent; and  $K_j$  is the global emitter coefficient used.

$N$  and  $\beta$  variables are two leakage model parameters that represent the influence of some factors on the relationship between leakage and pressure. Parameter  $\beta$  represents the pipe deterioration over time, thus it depends on both pipe characteristics and various external factors like mainly the average pressure, but there are also others such as environmental conditions or corrosion. In contrast,  $N$  is a function of pipe characteristics only (Adedeji et al., 2017; Laucelli and Meniconi, 2015). The value of  $\beta$  can be varied between  $10^{-4}$  and  $10^{-5}$  and  $N$  oscillates between 0.5 and 1.5. The model calibration enables the estimation of the ratio between real leaks and total leaks and  $N$  exponent (Ávila et al., 2021).

Step B.III develops the calibration leakages model. The calibration model distributes the leakages once the performances (i.e.,  $\eta_{AL}$ ,  $\eta_{RL}$ , and  $\eta_L$ ) are known. The model considers the following equation to evaluate the leakage in each element (i.e., line or tap):

$$q_{L,ij} = K_j (P_{ij})^N \quad (7)$$

where  $q_{L,ij}$  is the leakage flow for the element  $j$  (i.e., line or consumption point) at the time  $i$ ;  $P_{ij}$  is the pressure in the element  $j$  at the time  $i$  (if the element is a line, the chosen pressure is the average pressure value of the line -  $P_{ij} = \bar{P}_{ij}$ );  $N$  is the leakage exponent; and  $K_j$  is the global emitter coefficient. In this step the model determines the value of the global emitter coefficients assigned to lines and consumption points in different iterations, minimizing the error between simulated leakage volume and leakage volume of the water system.

The leakage volume is defined using the following expression:

$$V_{L,j} = \sum_{i=1}^{i=T} (q_{L,ij} \Delta t) = \sum_{i=1}^{i=T} (K_j (P_{ij})^N \Delta t) \quad (8)$$

where  $\Delta t$  is the interval time in s,  $V_{L,j}$  is the leakage volume for the element in  $\text{m}^3$ , assuming the  $K_j$  is constant in all annual simulations. It is defined by the following expression through an iterative procedure

$$K_j = \frac{V_{L,j}}{\sum_{i=1}^{i=T} ((P_{ij})^N \cdot \Delta t)} \quad (9)$$

The model calibrates the system by estimating  $K_j$ . It considers all elements of the water systems have leakages, therefore, the total leakage volume is distributed in the system. The leakage volume of each element ( $V_{L,j}$ ) can be determined by the following expression:

$$V_{L,j} = \delta_j V_L = \delta_j \eta_L V_I \quad (10)$$

where  $\delta_j$  is the distributed coefficient assigned to each element of the network. The addition of all distributed coefficients is equal to 1.  $\delta_j$  is estimated by Eq. (11) when it is applied to lines and Eq. (12) when it is used in tap

$$\delta_j = \frac{L_j}{\sum_{j=1}^{j=k} (L_j)} \quad (11)$$

$$\delta_j = \frac{V_{T,j}}{\sum_{j=1}^{j=m} (V_{T,j})} \quad (12)$$

where  $L_j$  is the length of the line  $j$  in m;  $k$  is the number of lines of the model. It depends on the material of the line.;  $k$  is the number of pipes;  $V_{T,j}$  is the total consumed volume of the consumption points ( $j$ ), including both measured (invoiced) for consumption as well as the leakage volume (no invoiced);  $m$  is the number of consumption points of the model.

Once the error is minimized, it should be verified if the KPI values are acceptable. If they are not acceptable, the hourly fitting curves (Input 8) should be used and the simulation and determination of the flow and pressures in pipes should be carried out again. The new fitting coefficient applied to all consumption nodes is defined by the following equation:

$$k_i = k_{i,0} \frac{Q_{i,\text{observed}} - Q_{i,\text{leakage}}}{Q_{i,\text{simulated}} - Q_{i,\text{leakage}}} \quad (13)$$

where  $k_i$  is the new fitting parameter at time  $i$ ,  $k_{i,0}$  is the ratio between  $Q_{i,\text{consumed},0}$  and  $Q_{i,\text{simulated},0}$ . It is used as a fitting coefficient in all consumption nodes;  $Q_{i,\text{consumed},0}$  is the estimated flow, which is consumed at the time  $i$  and it is defined by the difference between observed flow ( $Q_{i,\text{observed}}$ ) and average leakages flow ( $\bar{Q}_{\text{leakage},0}$ );  $Q_{i,\text{simulated},0}$  is the simulated flow when the leakages are not considered in the simulated model.

This calibration is developed using the EPANET toolkit (Rossman, 1999) to calibrate the leakage model (Step B.III). When the key performance indicators (KPIs) show acceptable values, the leak calibration ends, and the model is ready for energy balance. The used KPIs were bias percentage (PBIAS), Mean Relative Deviation (MRD), Root Mean Square Error (RMSE) and Mean Absolute Deviation (MAD).

1 PBIAS measures the tendency of the simulated values and establishes if the obtained values in the model are smaller or larger than the registered values. If PBIAS is less than zero, the proposed model overestimates the considered variable; if it shows positive values, it indicates the variable is underestimated, and finally, if the PBIAS value is zero, it indicates the model is optimal. PBIAS is defined by the following expression:

$$\text{PBIAS}(\%) = \frac{\sum_{i=1}^N (O_i - P_i)}{\sum_{i=1}^N O_i} \cdot 100 \quad (14)$$

where  $O_i$  are the registered values;  $P_i$  the experimental values and  $N$  the number of observations.

When PBIAS is lower than +/-10% the fitness is considered very good. If the PBIAS values are between +/-10 and +/-15%, the fitness is good. When the PBIAS value is between +/-15% and +/-25% the fitness is satisfactory and if it is higher than +/-25% it is considered unsatisfactory (Moriasi et al., 2007).

1 MRD. considers the weight of the error to the variable value. If MRD is zero, this value indicates a perfect fit. It is defined by the following expression:

**Table 1**  
Equations to define the annual energy balance in kWh.

Type	Equation ID
Total Energy ( $E_{T_J}$ )	$\gamma Q_j(z_o - z_i)$ (18)
Friction Energy ( $E_{FR_J}$ )	$\gamma Q_j(z_o - (z_j + P_j))$ (19)
Theoretical Energy Necessary ( $E_{TN_J}$ )	$\gamma Q_j P_{minj}$ (20)
Energy Required ( $E_{RS_J}$ )	$\gamma Q_j P_{minSj}$ (21)
Theoretical Available Energy ( $E_{TA_J}$ )	$\gamma Q_j (P_j - P_{minj})$ (22)
Theoretical Recoverable Energy ( $E_{TR_J}$ )	$\gamma Q_j (P_j - \max(P_{minj}; P_{minSj}))$ (23)
Theoretical Recoverable Energy ( $E_{TR_{mj}}$ )	$\gamma Q_j \eta_i H_i$ (24)

$$MRD = \sum_{i=1}^N \frac{|O_i - P_i| / P_i}{N} \quad (15)$$

2 RMSE is the index, which measures the error between the simulated values and recorded values. When RMSE is zero, this value indicates a perfect fit. It is defined by the following expression:

$$RMSE = \sqrt{\frac{\sum_{i=1}^N [O_i - P_i]^2}{N}} \quad (16)$$

3 MAD shows the absolute differences between simulated and recorded values. The perfect fit is defined when MAD is zero, and it is defined by the following expression:

$$MAD = \frac{\sum_{i=1}^N |O_i - P_i|}{N} \quad (17)$$

### 2.1.3. Energy Balance

Energy balance is crucial to estimate the distribution of the supplied energy in the different energy terms (i.e., required energy, losses, among others) (del Teso et al., 2019). When the energy balance is developed, the discretization of the different energy terms related to the pressure excess is possible. In this step the water managers can difference the terms for the available energy between the theoretically recoverable energy and the theoretically non-recoverable energy, considering the pressure and the minimum consumption at each point of consumption (Input 10) (Pérez-Sánchez et al., 2017).

The energy balance will allow us to estimate the recovered height of each flow over time, this would be the data pair ( $Q$ ,  $H$ ), managing to select the most appropriate machine at each study point (Input 11). Table 1 summarizes the different expressions to consider the energy balance.

( $E_{T_J}$ ) It is the total potential energy supplied to the system when it is not being consumed from the network.; ( $E_{FR_J}$ ) energy that is dissipated in the network from the point of departure to the point of consumption; ( $E_{TN_J}$ ) minimum energy required in the system to ensure that the minimum pressure established at the most unfavourable point of the

network is met; ( $E_{RS_J}$ ) it is the energy, for a time interval, necessary for the minimum pressure restriction to be fulfilled at a point; ( $E_{TA_J}$ ) for a time interval, it is the energy that is theoretically available to be recovered in a line; ( $E_{TR_J}$ ) is the maximum amount of theoretically recoverable energy at a point of consumption; ( $E_{TR_{mj}}$ ) energy that cannot be recovered in the network;  $Z_i$  is the geometric height above the reference plane of the point of consumption;  $Z_o$  is the geometric height above the reference plane of the free surface of the water in the tank that supplies the system in m;  $\gamma$  is the specific weight of the fluid in kN/m<sup>3</sup>;  $Q_j$  is the circulating flow;  $P_j$  is the pressure at a point;  $P_{min}$  is the minimum pressure that can exist at the point of consumption;  $H_i$  is the head level of the reservoir in m w.c.;  $\eta_i$  the efficiency of the recovery system for this flow  $Q_j$  (Rosado et al., 2020).

### 2.1.4. Recovery Analysis

The final block is defined by the recovery analysis. The objective of this phase is to determine the optimal location of the energy recovery points and the optimal definition of regulation strategies from a PATs database. In this section, a double annealing simulation procedure is carried out. The energy recovery analysis has two phases, called D.I Location Optimization and D.II Selection Optimization.

The location optimization process begins with the definition of the optimization functions, these objective functions are defined under (i) energy, (ii) hydraulic and (iii) economic criteria. These objective functions were the maximization of the theoretical recoverable energy ( $OF1 = E_{TR}$ ), the reduction of leaks in the distribution network ( $OF2 = \Delta V_L$ ); and the Levelized Cost of Energy ( $OF3 = LCOE$ ). This function only takes into account expenses (initial investment and annual costs) and it does not depend on energy prices.

$$OF3 = \frac{IC_0^T + \sum_{i=1}^{i=T} \frac{AC_i^T}{(1+k)^i}}{\sum_{i=1}^{i=T} \frac{E_i^T}{(1+k)^i}} \quad (25)$$

where  $IC_0^T$  is the initial investment in € in the year 0, considering the electric line to reach the supply points;  $AC_i^T$  is the operation and maintenance costs in € for the year  $i$ ;  $E_i^T$  is the annual recovered energy in kWh for the year  $i$ ;  $T$  is the lifecycle in years, considering 25 years;  $k$  is the discount rate using a sensitivity analysis between 0.01 and 0.1.

The research presented in (Pérez-Sánchez et al., 2018) proposed a methodology for maximizing energy recovery, assigning PATs in water networks through simulated annealing techniques for different objective functions and some machines. This heuristic search algorithm is based on the analogy with the physical process of annealing metals. The algorithm searches for the best locations for the recovery systems based on the defined objective functions as well as the number of recovery systems established. PATs were simulated on EPANET as a general-purpose valve in which the BEH, BPH or operational curve was defined in each iteration by EPANET Toolkit. The analysis was developed considering an simulation, which a demand dependent analysis (Rossman, 1999), therefore the demand is not dependent on the pressure but the leakages is influenced by pressure values.

The procedure requires defining the number of iterations and assigning control parameters to characterize the simulated annealing process. These parameters are the initial temperature ( $T_i$ ); the final temperature ( $T_f$ ); the cooling rate ( $\alpha_c$ ); and the number of transitions ( $L_0$ ) in each temperature step. These parameters are fixed according to a sensitivity analysis previously performed and they are changed depending on the objective maximized function (Ávila et al., 2021). Once the control parameters have been defined, the maximum number of recovery systems ( $N$ ) is determined. The procedure must consider the generation of the initial configuration. The methodology considers two recovery systems ( $m$ ) in the first two elements of the list initially. A new combination between different elements for each value of the recovery system ( $m$ ) is developed by the annealing procedure. Subsequently, the

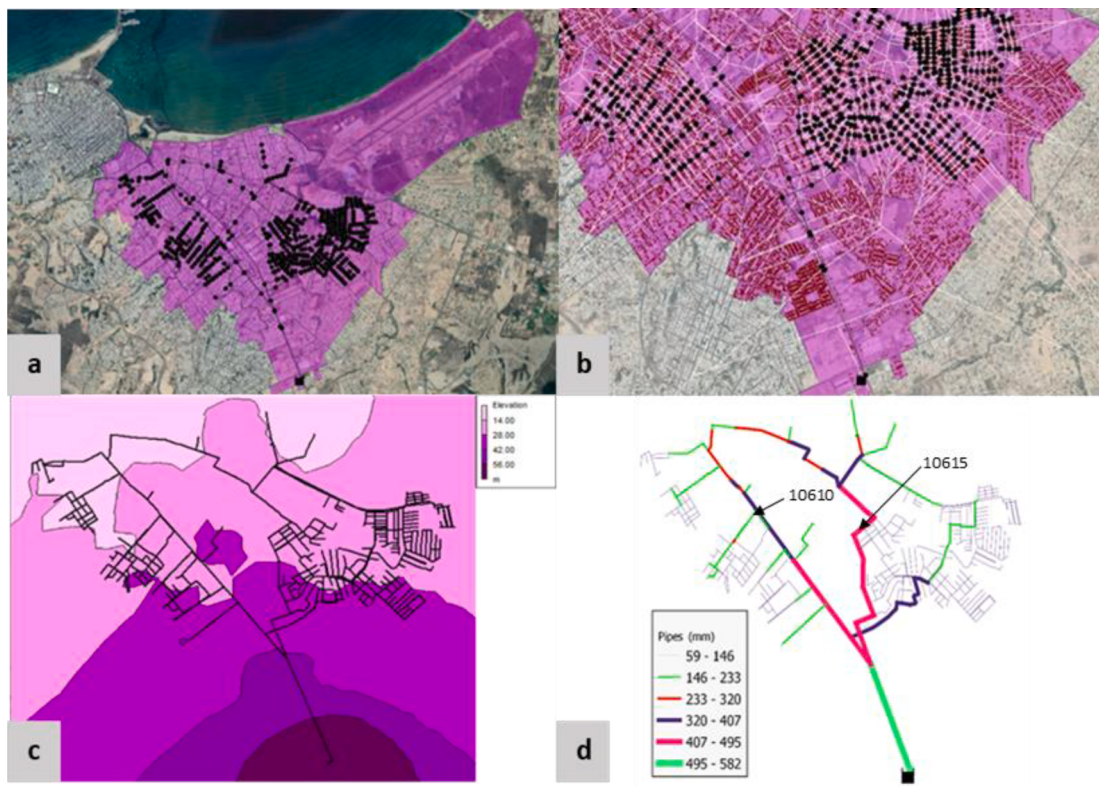


**Figure 2.** Characteristics of the hydraulic network of Manta. (a) Hydraulic network; (b) Network junctions and users; (c) Height difference in the network; (d) Pipe diameters and locations of two recovery systems.

optimization process establishes the best location and operating points for this value  $m$ . Finally, the result of this stage is to know the optimal configuration of the recovery system to start the last stage of this methodology, the selection optimization.

When step D.I is run and the location is chosen, the second phase (D.II) starts developing an optimized selection of the hydraulic machine. It consists of searching for the selection of the number of machines to be installed and the best regulation strategy according to the defined variables. These are defined based on the specific speed ( $\eta_{st}$ ), head and discharge number. These values enable the calculation of dimensionless parameters. To select the machine, the best efficiency point (BEP) from the database of 110 PATs is used. The definition of the operational curves is established according to the proposed methodology by Pérez-Sánchez et al. (2020). The knowledge of the characteristic curves implies the possibility to define the best regulation strategy considering the rotational variation speed and therefore, the methodology optimizes the key operation according to best efficiency head (BEH), best power head (BPH), Nominal Rotation (NR) or best power flow (BPF) according to the proposed method by Macías Ávila et al. (2021).

The success of the methodology requires an additional internal annealing simulation procedure, since the optimization process evaluates many combinations, such as (i) the possibility of using a different number of machines that could be installed in series or parallel; (ii) regulation strategies; (iii) and different numbers of possible recovery systems to be installed on the network. As a novelty, the methodology was modified to work in a meshed network. It involved the development of an internal iterative procedure to define the best machine and its regulation, once the located line was established. This iterative procedure is delimited as a function of the error value between iterations, considering both leakage reduction and recovered energy.

**Table 2**  
Network study data.

Network data and study area	Value
Area coverage	1991 ha
Population served (estimated)	100000
Number of metered properties	23885
Total pipe length	65 km
Average daily pressure (2021), estimated by Renaud et al. (2012)	35.14 m
Nonrevenue water (January and February)	43%
Junctions	832
Pipes	875
Maximum level difference	59 m
Diameter range	59 - 581mm
Pipe materials	PVC

## 2.2. Case Study. Manta (Ecuador) water distribution system

The proposed methodology was applied to the case study of the city of Manta, Ecuador. The model of the water supply network is shown in Fig. 2a. The drinking water network that supplies 110 neighbourhoods in the city of Manta, provides the flow from a reservoir, which its level is 65 m. There is a flowmeter and it is installed in the main pipe and its main function is the measure the flow supplied to the system. Fig. 2b shows the red dots, which represent different consumption nodes. The topology of the network, the height and consumption of the different junctions, the consumption patterns, the recorded values of the flowmeter and the recording of the meters, which are recorded each month. All data are referred to as 2021. The model was developed using EPANET software, using 832 nodes, 875 lines and 1707 virtual leakages nodes. It was established an hourly consumption pattern to develop an hourly energy analysis and water volume evaluation in terms of leakages.

Fig. 2c shows the orography of the study area using a contour map of the heights of the network. The highest point is in the reservoir, while

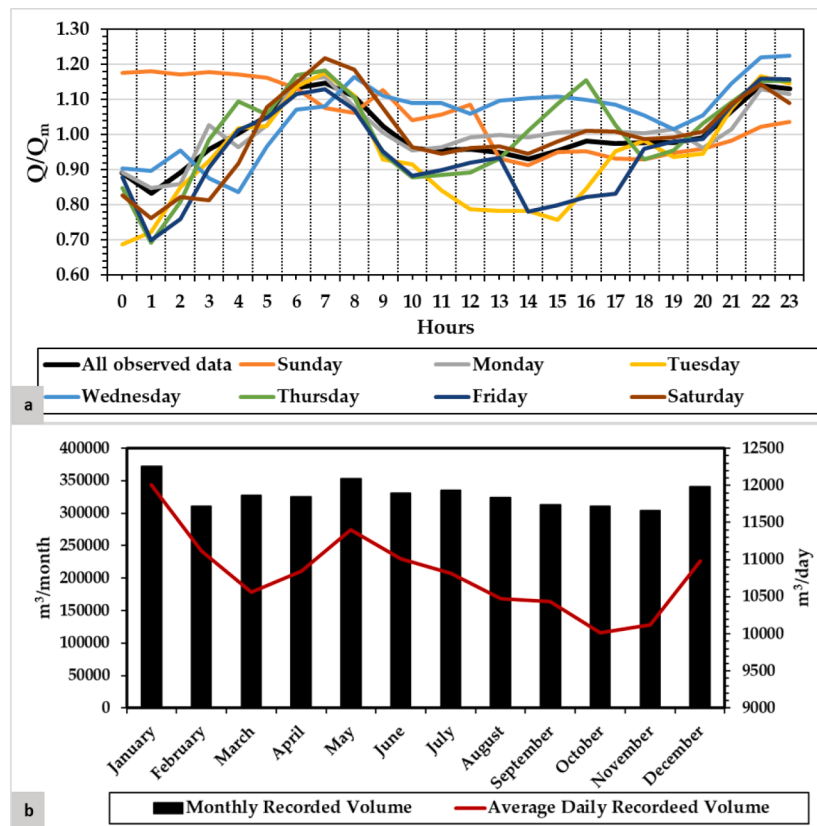


**Figure 3.** (a) Daily consumption pattern ( $Q_m$  is the average flow) ( $\text{m}^3$ ); (b) Data of the recorded volume of the network in the year 2021.

the lowest is in the branches of the network. The material of the pipes is polyvinyl chloride (PVC). The pipe diameters of the network are shown in Fig. 2d. These diameters vary from 581mm in the main branches to 59mm in the secondary ones. Table 2 shows the main data of the case study as well as the characteristics of the hydraulic network.

The network is supplied through a tank, this contains a flow meter in its discharge with flow data every fifteen minutes. This study used recorded values for January and February 2021. Both months showed a similar flow trend since the climatic conditions are similar over time and the city is not touristic, being constant the number of citizens. The maximum registered flow supplied to the network was 543 l/s, the minimum flow was 92 l/s and the average flow was 231 l/s when January was analyzed. When February is analyzed, the maximum flow was 632 l/s, the minimum flow was 91 l/s and the average flow was 246 l/s.

Fig. 3 shows the consumption data provided by the management company for the year 2021. The average daily consumption for each of the months of the year varies from 10011 to 12005  $\text{m}^3$ . The consumed volume is the highest in January and it is the lowest in November.

Fig. 3a shows the daily variation of the water pattern consumption. The highest value was located between 5 and 7 am. Besides, there was a peak between 8 and 10 pm. The lowest value was located between 12 am and 3 am. The monthly recorded volume in the network varied between 303782 and 372168  $\text{m}^3$  (Fig. 3b). If the injected volume in the network is analyzed, this annual volume was 6925926  $\text{m}^3$ , and the recorded volume was 3947778  $\text{m}^3$ . In this case, the leak percentage was equal to 43% and the average leakage flow was 92.61 l/s.

### 3. Results

The analysis to discretize leakages between apparent and real losses was developed as a first step, once the model was established. The discretization of the leaks was necessary to calibrate the model. Knowing

the registered volume by counters and the registered volume by the installed flowmeter in the mainline, seven hypotheses were developed in the sensitivity analysis establishing differences between real and apparent losses. Each hypothesis is defined in Figures from 4a to 4d.

It is identified by  $Hx(y;z)$  in which “ $x$ ” is the number of the hypothesis, “ $y$ ” is the weight of the apparent losses and “ $z$ ” is the weight of the real losses. This analysis was considered for the different error indexes defined in the methodology. Previously in Step B.II, a first calibration of the  $\alpha$  coefficient was established considering the leakages (43%). This value was 0.65 since all values of  $\beta$  coefficient, which oscillate between  $10^{-5}$  and  $10^{-4}$  are lower than the limit of leaks percentage.

Fig. 4a shows the results when PBIAS was analysed for the different seven hypotheses, considering six different time intervals. The PBIAS value was between 5.274 and 5.554 for the different 42 scenarios. All cases showed excellent fit according to Moriasi et al. (2007). To simulate the definitive model, H4 was chosen since it showed the lowest PBIAS value. H4 also showed the best values for the rest of KPIs. Finally, an hourly interval was chosen to develop the simulation. RMSE, MAD and MRD were also established for the different scenarios. If the hourly interval is analysed, RMSE was 42.6 (Fig. 4c), MAD was 17.36 (Fig. 4d) and the MRD was 0.118 (Fig. 4b). This calibrated model showed the following error between simulated and registered volume (Table 3). The error was defined by the following expression:

$$\epsilon_V = \frac{(V_{\text{simulated}} - V_{\text{registered}})}{V_{\text{registered}}} \cdot 100 \quad (26)$$

Fig. 4e shows the example of the visual trend between registered and simulated flow in the calibrated model, which used H4 to establish the apparent and real losses and was used to develop the energy balance and the optimization procedure. Table 3 shows the monthly error between the registered and simulated volume. These errors were below 1.5% in all months, considering an average annual error equal to 0.55%. A

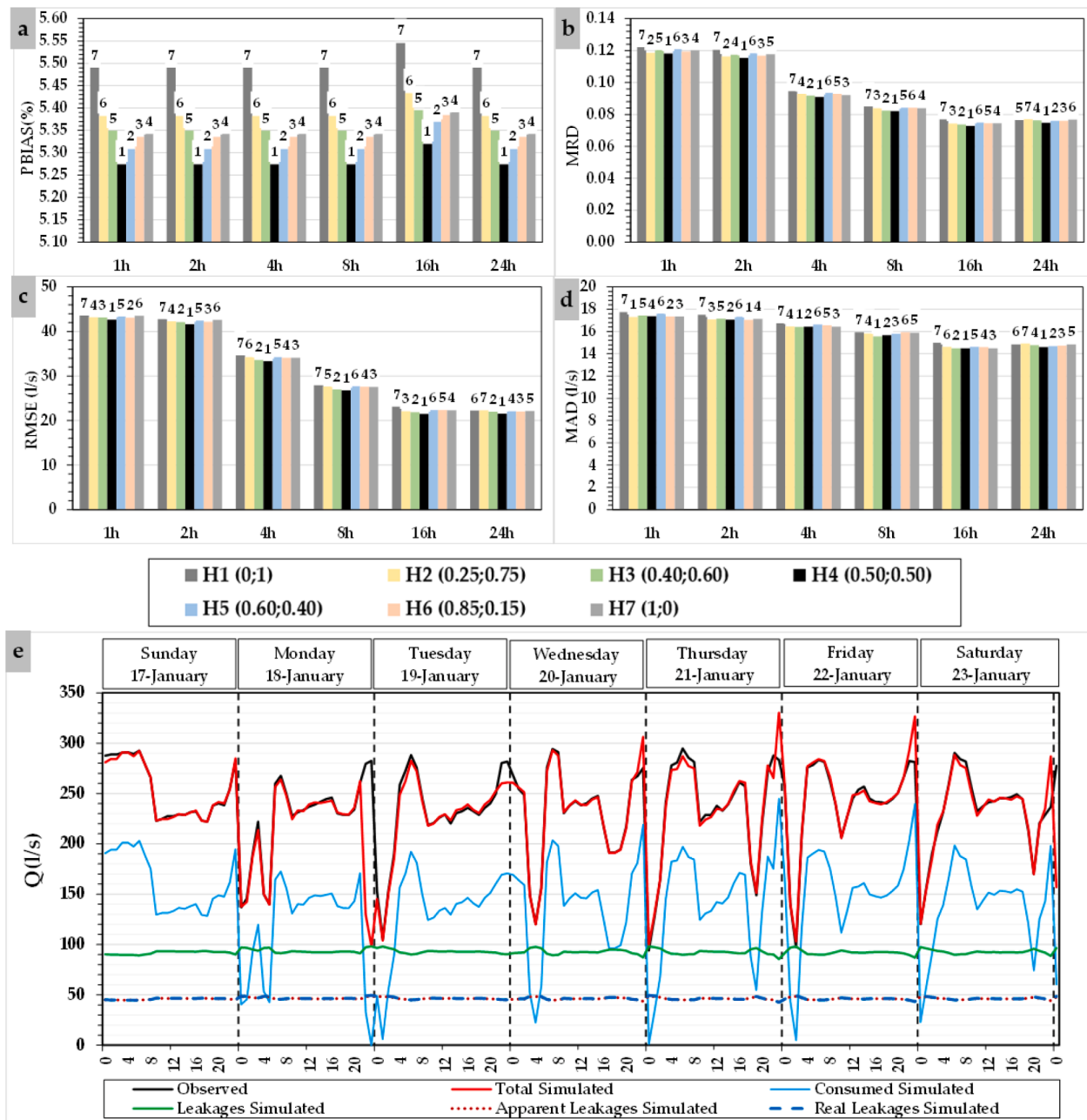


**Figure 4.** (a) Calibration leakages considering PBIAS value; (b) Calibration leakages considering MRD values; (c) Calibration leakages considering RMSE; (d) Calibration leakages considering MAD; (e) Comparison between observed flow and simulated values when the model was calibrated. Example of one week.

double calibration is performed. The first calibration takes place in Step A, and consists of comparing the monthly and annual volumes observed in the user meters with a hydraulic model that only takes into account the demand (without leaks). The second calibration is performed in Step B. It consists of comparing the observed values of the main flowmeter for January and February with the hydraulic model that takes into account leakage. For each calibration, the different inputs are modified minimizing the errors and finally determining the hypothesis of weight distribution for real and apparent leakage that minimizes the values for the KPIs.

The first optimization procedure established the best lines to install recovery systems as a function of the objective function. The optimization worked using minimum pressure, which must be guaranteed in any scenario.

Table 4 shows the chosen lines according to the three different objective functions. This first optimization procedure enabled the

definition of the best location, the energy and leakages volume are further compared with the final values when the machines will be selected. When the case study was analysed using the OF1, the theoretical annual recovered energy oscillated between 47507 and 104123 kWh depending on the used recovery systems (Fig. 5a). The leak reduction varied from 206792 to 379652 m<sup>3</sup> (Fig. 5b) and LCOE value from 0.186 to 0.264 €/kWh (Fig. 5c). In all cases, the incorporation of the new lines to install the recovery system influenced the variation of the variable by around 30% when the second recovery system was added. A similar trend showed the incorporation of the fifth unit, which increased or reduced the variable by around 10%. When OF2 and OF3 were analysed in this D.I step, the results were similar but the lines were different.

Finally, the chosen OF was the OF1 because it shows similar leakage reduction values and the LCOE values were acceptable to focus the selection of the machine in those lines where the recovered energy will be

**Table 3**

The error between registered and simulated volume, considering H4 in the mainline of the water system.

Month	Registered Volume (m <sup>3</sup> )	Simulated Volume (m <sup>3</sup> )	Error (%)
January	372168	369734.02	-0.65%
February	311329	309521.17	-0.58%
March	327354	324714.44	-0.81%
April	325230	321086.32	-1.27%
May	353607	352251.86	-0.38%
June	330395	329607.30	-0.24%
July	335415	333407.18	-0.60%
Agost	324746	323471.30	-0.39%
September	312938	311696.57	-0.40%
Octuber	310334	309808.83	-0.17%
November	303782	300630.52	-1.04%
December	340479.5	340115.43	-0.11%
Annual	3947777.5	3926044.94	-0.55%

higher. However, any OF could be chosen to develop the D.II step, comparing the results.

Fig. 5 shows the information shown in Table 4 in terms of energy (Fig. 5a), Leakage reduction (Fig. 5b), LCOE values (Fig. 5c) and generated power (Fig. 5d). These figures show the results obtained in the optimization grouped by OF according to the number of lines installed and the pumps operating as turbines.

**Table 4**

Preliminary results when D.I step is defined to locate the best line.

OF	Line 1	Line 2	Line 3	Line 4	Line 5	E (kWh)	Leakages Reduction (m <sup>3</sup> )	LCOE (€/kWh)	P (kW)
OF1	10615					47507	206792	0.186	8.18
OF1	10615	10610				66163	282333	0.216	12.15
OF1	10026	10222	10610			83355	313553	0.206	14.88
OF1	10026	10610	10615	10618		94069	350492	0.244	19.58
OF1	10026	10208	10222	10610	10618	104123	379652	0.264	24.42
OF2	10620					46250	210204	0.190	8.05
OF2	10620	10591				62789	289398	0.228	12.19
OF2	10227	10591	10615			70839	339118	0.307	16.94
OF2	10013	10266	10591	10620		86843	375039	0.262	20.14
OF2	10013	10266	10591	10620	10663	96533	409669	0.294	24.62
OF3	10942					18173	36206	0.163	2.88
OF3	10222	10794				43432	119888	0.207	8.28
OF3	10013	10266	10971			57209	199560	0.204	11.51
OF3	10013	10266	10620	10942		83387	341547	0.227	17.79
OF3	10224	10237	10708	10794	10971	89506	325469	0.242	21.23

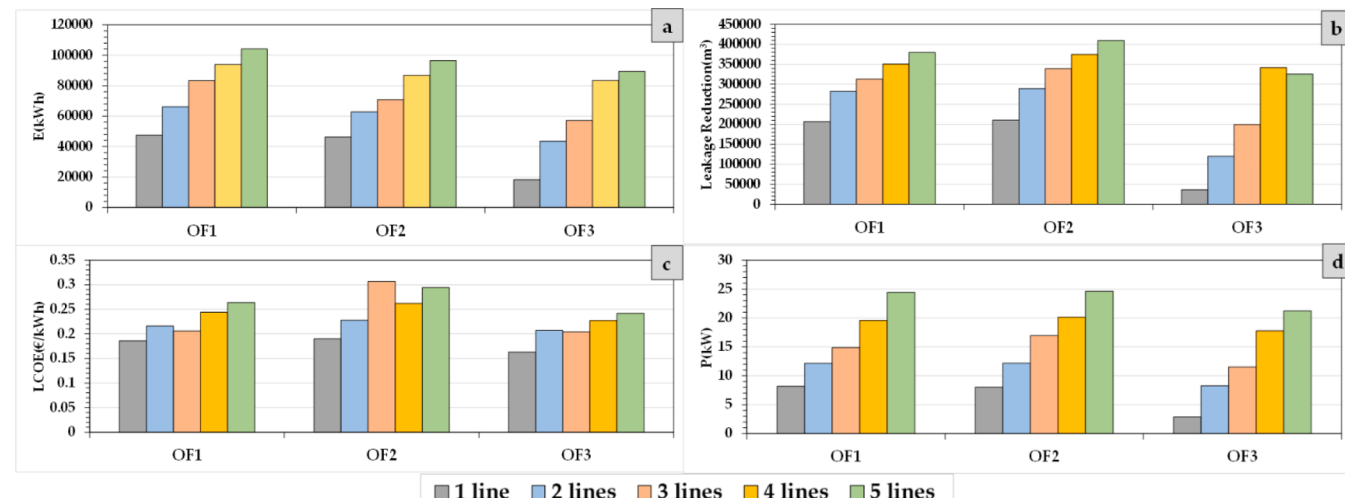


Figure 5. (a) Annual recovered energy; (b) Leakages reduction; (c) LCOE values; (d) Generated power

**Table 5**

Optimized results when the methodology is considered using a recovery system alone.

Iteration	1	2	3	4	5
Configuration	1	1	1	1	1
Line	10615	10615	10615	10615	10615
ID	128	128	128	128	128
$n_{st}$ (rpm) [m, kW]	23.51	23.51	23.51	23.51	23.51
$N_m$	3	3	3	3	3
D(mm)	400	400	400	400	400
N (rpm)	750	750	750	750	750
$Q_{BEP}$ (l/s)	62.64	62.64	62.64	62.64	62.64
$H_{BEP}$ (m w.c.)	15.95	15.95	15.95	15.95	15.95
SR (Strategy Regulation)	NR	NR	NR	NR	NR
Annual $E_{TR}$ (kWh)	52491.91	23746.4	23565.06	23572.44	23624.93
Leakage reduction ( $m^3$ )	96102.9	96567.19	96722.75	96358.64	96725.92
LCOE ( $\text{€}/m^3$ )	0.233	0.1605	0.1659	0.1678	0.1574
P (kW)	14.83	14.98	15.95	16.42	14.04
Energy difference (%)	54.76%	0.76%	-0.03%	-0.22%	
Leakage reduction difference (%)	-0.48%	-0.16%	0.38%	-0.38%	

**Table 6**

Optimized results when methodology is considered using two recovery systems.

Iteration	1	2	3	4	5	6
Configuration	2	2	2	2	2	2
Line	10615	10610	10615	10610	10615	10610
ID	49	30	128	30	83	54
$n_{st}$ (rpm) [m, kW]	26.68	18.58	23.51	18.58	23.51	31.63
$N_m$	3	3	3	3	3	3
D(mm)	300	300	400	300	300	300
N (rpm)	750	750	750	750	1200	750
$Q_{BEP}$ (l/s)	53.612	23.31	62.64	23.31	42.28	37.12
$H_{BEP}$ (m w.c.)	12.154	11.3	15.95	11.3	22.98	7.58
SR (Strategy Regulation)	BEH	NR	NR	NR	BEH	BEH
Annual $E_{TR}$ (kWh)	62317.2	41832.661	41279.3	29911.87	35483.76	34490.44
Leakage reduction ( $m^3$ )	131251.72	115013.23	128828.66	124425.54	122949.00	120245.8
LCOE ( $\text{€}/m^3$ )	0.271	0.201	0.22	0.337	0.286	0.189
P (kW)	19.25	28.62	22.63	62.11	63.87	26.66
Energy difference (%)	32.87%	1.32%	27.54%	-18.63%	2.80%	
Leakage reduction difference (%)	12.37%	-12.01%	3.42%	1.19%	2.20%	

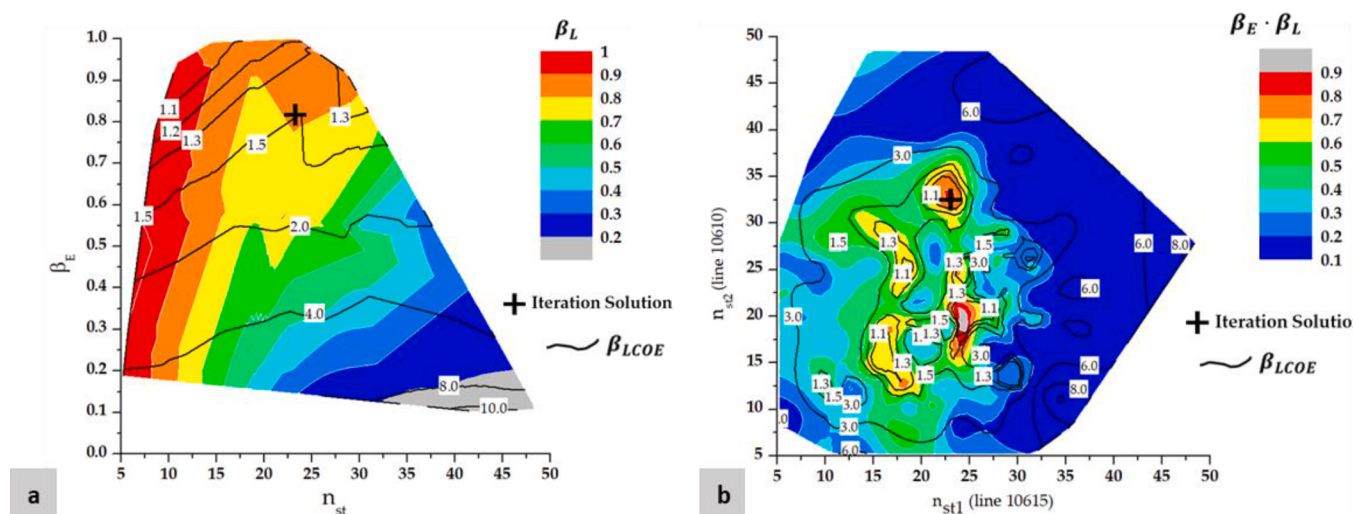


Figure 6. (a) Iteration solution when a recovery system was installed. (b) Iteration solution when two recovery systems were analysed.

difference between the last iterations is analyzed the energy and leakage reduction was 0.22 a 0.38%, respectively, therefore, the recovery system was established when the methodology stopped. The final energy and leakages values decreased by 50% compared with the preliminary simulated annealing (Table 4), which is considered the ideal machine to operate in the system.

Table 6 shows the results when two recovery system was analyzed. In this case, lines 10615 and 10610 were optimized as a function of the results shown in Table 4 when the OF1 was analyzed. The use of two recovery systems showed the variation of the typology of the machine as well as the BEP of these machines varied until reached the fifth iteration in the optimized procedure.

The selected machines were defined by a specific value of 23.51 and 31.63 rpm (m, kW) for lines 10615 and 10610 respectively. The BEP defined in the database was 42.28 l/s and 22.98 m w.c. for line 10615. When line 10610 was optimized, the BEP was 37.12 l/s and 7.58 m w.c. In both cases, the strategy of the regulation was the best efficiency head (BEH) and the number of used machines in parallel was three. The final annual recovered energy was 34490 kWh. This value was 52.4% of the estimated energy in the first optimization procedure to choose the best location (Table 4). When the leakage value was observed, its reduction was 120246  $m^3$  (42.58 % compared to the maximum reduction using simulated annealing in ideal conditions in Table 4, Step D.I)

The LCOE values were feasible in both cases according to feasible limits defined by (Lugauer et al., 2021). When one recovery machine was analyzed the LCOE value was 0.157  $\text{€}/m^3$ . If two recovery systems

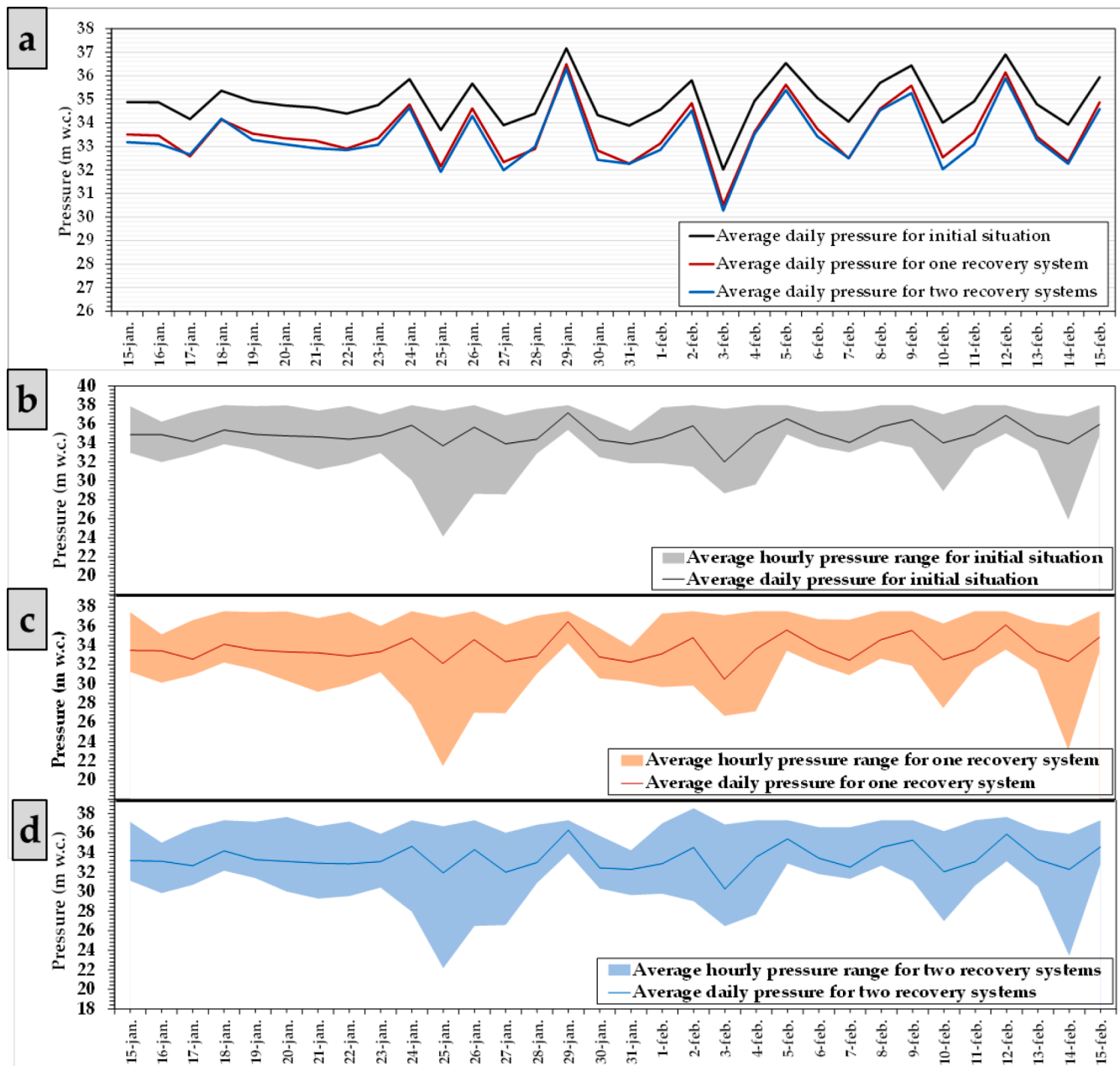


**Figure 7.** (a) Average daily pressure. (b) Average hourly pressure range for the initial situation; (c) Average hourly pressure range for one recovery system; (d) Average hourly pressure range for two recovery systems.

are installed, this value was  $0.189 \text{ €}/\text{m}^3$ . Fig. 6a shows the results related to Table 5 when a recovery system was analyzed in the water network as a function of the specific speed of the machine. The figure shows the best solution compared with the available ratios. These ratios were energy ratio ( $\beta_E$ ), which defines the ratio between the recovered energy between maximum recovered energy, the LCOE ratio ( $\beta_{LCOE}$ ), which defines the ratio between LCOE and minimum LCOE and Leakages ratio ( $\beta_L$ ), which defines the ratio between the reduction leakages and maximum reduction leakages. Fig. 5a shows this interaction in the best solution reaching an energy ratio of 0.78,  $\beta_L = 0.92$  and  $\beta_{LCOE} = 1.5$ .

Fig. 6b shows the integration of the best solution when two recovery systems were analysed in which the results are linked to Table 6. The figure shows the best solution is located on the best hill on the contour map. This case shows the interaction between  $\beta_E\beta_L$  and the  $\beta_{LCOE}$ , reaching values of 0.8 and 1.1 respectively. Both figures showed the proposed methodology of the optimization established the best solution

possible considering the available database of PATs and the constraints of the water system. The proposed solution implied a reduction of 96726 and 120246  $\text{m}^3$  when one or two recovery systems were analysed respectively. The average pressures were calculated according to Renaud et al. (2012), using a hydraulic model and weighting according to node elevations. The maximum pressure was 37.98, 37.59 and 38.56 m w.c. for the initial situation, one recovery system and two recovery systems, respectively. The minimum pressure values were 12.99, 10.78 and 11.47 m w.c. for the initial situation, one recovery system and two recovery systems, respectively. The average pressure en in the system when initial situation, one recovery system and two recovery systems were analysed, they were 35.15, 33.86, 33.61 m w.c., respectively.

Fig. 7 shows the variation of the pressure over time. It shows a monthly example between 15th January and 15th February for the initial situation of the water system, the scenario of the model considering one recovery system installed in the model and the second

**Table 8**

Improvement of the different sustainable indicators.

Type	Abbreviation	Definition	Indicator	Units	Initial Situation	1 Recovery System	2 Recovery Systems
Energy	IED	Ratio between friction energy and input energy	Energy dissipation	Dimensionless	0.088	0.160	0.178
	IAE	Sum of the total active energy consumed in the network	Annual consumed energy	kWh	600483.38	592677.41	590717.91
	IEFW	Ratio between the active energy consumed and the total volume of water introduced in the system	Consumed energy per unit volume	kWh/m <sup>3</sup>	0.088	0.088	0.088
	IER	Sum of total energy recovered in the network	Annual Recovered Energy	kWh	0	23624.93	34490.44
	ERP	Recoverable energy percentage used of the total energy consumed in the system	Recoverable energy percentage	%	0	3.99	5.84
	IAAE	Sum of the total active energy consumed in the network subtracted by the sum of the total energy recovered in the network	Absolute annual consumed energy	kWh	600483.38	569052.48	556227.47
	IAEFW	Ratio between IAAE and the total volume of water introduced in the network	Absolute consumed energy per unit volume	kWh/m <sup>3</sup>	0.088	0.084	0.083
Economic	IRLGP	Ratio between reduction of the leakage volume for each installed power.	Water recovery per unit volume per installed energy.	m <sup>3</sup> /kW	0	6889.31	4510.35
	REC	Product of the cost of the electricity tariff per kWh of energy produced	Cost of recoverable electrical energy per installation of PATs (1)	€	0	4724.99	6898.09
Environmental	CWSBRL	Product of the cost of each cubic meter of water for each covered meter of water saved.	Cost of water saved by reducing leaks when installing PATs (2)	€	0	24181.48	30061.45
	CDRPE	Ratio between the reduction of CO <sub>2</sub> emission by the production of each kWh of renewable energy	Carbon Dioxide reduced by produced energy (3)	Tn	0	11.58	16.9
	CDRBL	Ratio between the reduction of CO <sub>2</sub> emission for each cubic meter of water saved by leaks.	Carbon dioxide reduced by each cubic meter of water saved by leaks	kgr CO <sub>2</sub> /m <sup>3</sup>	0	0.12	0.14

(1) 0.2 €/kWh; (2) 0.25 €/m<sup>3</sup>; (3) 0.49 kg/kWh (De Marchis et al., 2016).

scenario, which analysed the installation of the two recovery systems.

The inclusion of these new technologies implied the improvement of the different indicators. In this sense, different indicators were used to show the variation of these indicators in the different iterations and the final decision of the optimization procedure. The results are shown in Table 8.

Both economical, energy and environmental indicators improved. Therefore, the inclusion of the use of green recovery systems improves the management of the supply systems and it contributes to increasing the sustainability of the cities. Interesting results are shown in Table 4 and they are very interesting from the point of view of reducing water losses, although IRLGP is lower. It is mainly because the increase in power is greater than the increase in leakage reduction. For example, when two recovery systems were analyzed, the power increases by almost 50% while the increase in leakage reduction is only 25%, so the IRLGP index is lower.

#### 4. Conclusions

The improvement of the sustainability of the water distribution networks is key to achieving the different sustainable development goals. This challenge should be confronted by water managers of the cities to increase the efficiency, sustainability and reach of the different targets of the 2030 Agenda.

This research proposes a new strategy to improve the location of green energy recovery systems in the water distribution system. This proposal established an optimization procedure based on discretized hourly analysis along year. The methodology integrated different simulated annealing strategies to locate, select and regulated the best hydraulic machine as a function of the recovered energy, leakages reduction and economical terms (LCOE values) in a meshed network. As a novelty, the proposal also included a self-calibration, which enables the definition of a model characterizing the consumed volume, real leakages and apparent leakages of the network based on injected flow and consumption recorded by the water company.

The methodology was implemented in a real case study located in Manta (Ecuador). The methodology used the recorded data for the year 2021 to analyse the behaviour of the system when green energy recovery systems are implemented in the system. The analysis showed the real possibility to recover energy by improving the performance indicators of the water system. The analysis showed the annual reduction of leakages could be more than 120000 m<sup>3</sup>. When the ratio between reduction of the leakage volume for each installed power (IRLGP index) was estimated, it was equal to 4510 m<sup>3</sup>/kW. The proposed methodology is limited in the consideration of the monthly consumed volume to calibrate the leakages. This limitation could be adapted for calibrating the leakages according to flow over time in future developments if the water systems had installed remote meter reading systems to increase the number of recording users (e.g., daily or hourly) and more flow meters in the network that could sectorize and discretize it in the analysis.

The use of similar methodologies enable the development of a database of sustainable indicators, and therefore, the different hydraulic system could be classified and compared with each other. Access to this information will be rewarding for other water managers and it will contribute to the management of the different water resources. It will help to establish tools in the different cities. These tools enable the gradual incorporation of sustainable methodologies in water management. The use of sustainable indicators, which enable the definition of the new goals in the management of the water supply will establish the next challenge for the green cities, mainly in developing countries, which show high ranges of improvement.

#### CRediT authorship contribution statement

**Carlos Andrés Macías Ávila:** Validation, Formal analysis, Writing – original draft, Writing – review & editing. **Francisco-Javier Sánchez-Romero:** Conceptualization, Methodology, Software, Validation, Formal analysis. **P. Amparo López-Jiménez:** Writing – original draft, Writing – review & editing, Supervision. **Modesto Pérez-Sánchez:** Conceptualization, Methodology, Software, Validation, Formal analysis,

Writing – original draft, Writing – review & editing.

## Declaration of Competing Interest

The authors declare no conflict of interest.

## Fundings

Grant PID2020-114781RA-I00 funded by MCIN/AEI/ 10.13039/501100011033

## References

- Jing Niu, W., & Kai Feng, Z. (2021). Evaluating the performances of several artificial intelligence methods in forecasting daily streamflow time series for sustainable water resources management. *Sustain. Cities Soc.*, 64, Article 102562. Jan.
- Islam, M. S., & Babel, M. S. (2013). Economic analysis of leakage in the Bangkok water distribution system. *J. Water Resour. Plan. Manag.*, 139(2), 209–216.
- Bibri, S. E., & Krogstie, J. (2017). Smart sustainable cities of the future: An extensive interdisciplinary literature review. *Sustain. Cities Soc.*, 31, 183–212. May.
- Farley, M. (2001). Leakage Management and Control. *Who*, 1–98.
- Beuken, R. H. S., Lavooij, C. S. W., Bosch, A., & Schaap, P. G. (2007). Low leakage in the Netherlands confirmed. *8th Annu. Water Distrib. Syst. Anal. Symp.*, 2006, 174.
- Lambert, A. O. (2002). International Report: Water losses management and techniques. *Water Sci. Technol. Water Supply*, 2(4), 1–20.
- Liemberger, R., & Wyatt, A. (2019). Quantifying the global non-revenue water problem. *Water Sci. Technol. Water Supply*, 19(3), 831–837.
- Li, R., Huang, H., Xin, K., & Tao, T. (2015). A review of methods for burst/leakage detection and location in water distribution systems. *Water Supply*, 15(3), 429–441. Jun.
- Samir, N., Kansoh, R., Elbarki, W., & Fleifle, A. (2017). Pressure control for minimizing leakage in water distribution systems. *Alexandria Eng. J.*, 56(4), 601–612.
- Schwaller, J., Van Zyl, J. E., & Kabaasha, A. M. (2015). Characterising the pressure-leakage response of pipe networks using the FAVAD equation. *Water Sci. Technol. Water Supply*, 15(6), 1373–1382.
- Deyi, M., Van Zyl, J., & Shepherd, M. (2014). Applying the FAVAD concept and leakage number to real networks: A case study in Kwadabeka, South Africa. *Procedia Eng.* 89, 1537–1544.
- Lambert, A., Fantozzi, M., & Shepherd, M. (2017). Pressure: Leak flow rates using FAVAD: An improved fast-track practitioner's approach. In *CCWI 2017 - 15th Int. Conf. Comput. Control Water Ind.* September.
- Lambert, A. (2000). What Do We Know About Pressure: Leakage Relationships in Distribution Systems? *IWA Conf. Syst. Approach to Leakage Control Water Distrib. Syst.*, 1–8.
- Ferraiuolo, R., De Paola, F., Fiorillo, D., Caroppi, G., & Pugliese, F. (2020). Experimental and numerical assessment of water leakages in a PVC-A pipe. *Water (Switzerland)*, 12 (6).
- Serafeim, A. V., Kokosalakis, G., Deidda, R., Karathanasi, I., & Langousis, A. (2022). Probabilistic Minimum Night Flow Estimation in Water Distribution Networks and Comparison with the Water Balance Approach: Large-Scale Application to the City Center of Patras in Western Greece. *Water (Switzerland)*, 14(1).
- AL-Washali, T., Sharma, S., AL-Nozaily, F., Haidera, M., & Kennedy, M. (2018). Modelling the leakage rate and reduction using minimum night flow analysis in an intermittent supply system. *Water (Switzerland)*, 11(1).
- Canto Ríos, J., Santos-Tellez, R. U., Hansen Rodríguez, P., Antúnez Leyva, E., & Nava Martínez, V. (2014). Methodology for the identification of apparent losses in water distribution networks. *Procedia Eng.* 70, 238–247.
- Lambert, A. O., Brown, T. G., Takizawa, M., & Weimer, D. (1999). A review of performance indicators for real losses from water supply systems. *J. Water Supply Res. Technol. - AQUA*, 48(6), 227–237.
- Adedejì, K. B., Hamam, Y., Abe, B. T., & Abu-Mahfouz, A. M. (2017). Burst leakage-pressure dependency in water piping networks: Its impact on leak openings. *2017 IEEE AFRICON Sci. Technol. Innov. Africa, AFRICON 2017*, 1502–1507. no. September.
- Schwaller, J., & van Zyl, J. E. (2015). Modeling the Pressure-Leakage Response of Water Distribution Systems Based on Individual Leak Behavior. *J. Hydraul. Eng.*, 141(5), Article 04014089.
- Wu, S., Yang, L., Zhou, C., & Zhang, J. (2013). Leakage modeling and leakage control analysis by pressure management in water supply system of DMA. In *ICPTT 2013 Trenchless Technol. - Best Choice Undergr. Pipeline Constr. Renewal, Proc. Int. Conf. Pipelines Trenchless Technol* (pp. 141–150).
- Gupta, A., Bokde, N., Marathe, D., & Kulat, K. (2017). Leakage Reduction in Water Distribution Systems with Efficient Placement and Control of Pressure Reducing Valves Using Soft Computing Techniques. *Eng. Technol. Appl. Sci. Res.*, 7(2), 1528–1534. Apr.
- G. Ferrarese, S. Benzi, M. M. A. Rossi, and S. Malavasi, "Experimental characterization of a self-powered control system for a real-time management of water distribution networks," <https://doi.org/10.1080/1573062X.2021.1992453>, vol. 19, no. 2, pp. 208–219, 2021.
- Patelis, M., Kanakoudis, V., & Gonelas, K. (2017). Combining pressure management and energy recovery benefits in a water distribution system installing PATs. *J. Water Supply Res. Technol. - AQUA*, 66(7), 520–527.
- Lima, G. M., Luvizotto, E., & Brentan, B. M. (2017). Selection and location of Pumps as Turbines substituting pressure reducing valves. *Renew. Energy*, 109, 392–405.
- Ebrahimi, S., Riasi, A., & Kandi, A. (2021). Selection optimization of variable speed pump as turbine (PAT) for energy recovery and pressure management. *Energy Convers. Manag.*, 227, Article 113586. November 2020.
- Rossi, M., Nigro, A., Pisaturo, G. R., & Renzi, M. (2019). Technical and economic analysis of Pumps-as-Turbines (PaTs) used in an Italian Water Distribution Network (WDN) for electrical energy production. *Energy Procedia*, 158, 117–122.
- Fecarotta, O., & McNabola, A. (2017). Optimal Location of Pump as Turbines (PATs) in Water Distribution Networks to Recover Energy and Reduce Leakage. *Water Resour. Manag.*, 31(15), 5043–5059.
- Cimorelli, L., D'Aniello, A., Cozzolino, L., & Pianese, D. (2020). Leakage reduction in WDNs through optimal setting of PATs with a derivative-free optimizer. *J. Hydroinformatics*, 22(4), 713–724.
- Nguyen, K. D., Dai, P. D., Vu, D. Q., Cuong, B. M., Tuyen, V. P., & Li, P. (2020). A MINLP model for optimal localization of pumps as turbines in water distribution systems considering power generation constraints. *Water (Switzerland)*, 12(7).
- Giudicianni, C., Herrera, M., di Nardo, A., Carravetta, A., Ramos, H. M., & Adeyeye, K. (2020). Zero-net energy management for the monitoring and control of dynamically-partitioned smart water systems. *J. Clean. Prod.*, 252, Article 119745. Apr.
- Fontana, N., Asce, M., Marini, G., & Creaco, E. (2021). Comparison of PAT Installation Layouts for Energy Recovery from Water Distribution Networks. *J. Water Resour. Plan. Manag.*, 147(12), Article 04021083. Sep.
- Latifi, M., et al. (2021). Pressure and Energy Management in Water Distribution Networks through Optimal Use of Pump-As-Turbines along with Pressure-Reducing Valves. *J. Water Resour. Plan. Manag.*, 147(7), Article 04021039. May.
- Grupo Especialista en Benchmarking y Evaluación del Desempeño de la IWA, *Manual de Buenas Prácticas. Indicadores de Desempeño para Servicios de Abastecimiento de Agua - Tercera Edición*. 2018.
- Winarni, W. (2009). Infrastructure Leakage Index (ILI) as Water Losses Indicator. *Civ. Eng. Dimens.*, 11(2), 126–134.
- Ávila, C. A. M., Sánchez-Romero, F. J., López-Jiménez, P. A., & Pérez-Sánchez, M. (2021). Optimization tool to improve the management of the leakages and recovered energy in irrigation water systems. *Agric. Water Manag.*, 258.
- Almazan, J., Cabrera, E., Arregui, F., CabreraJr, E., & Cobacho, R. (2005). Leakage Assessment through Water Distribution Network Simulation. *J. Water Resour. Plan. Manag.*, 131(6), 458–466. Nov.
- Adedejì, K. B., Hamam, Y., Abe, B. T., & Abu-Mahfouz, A. M. (2017). Leakage detection and estimation algorithm for loss reduction in water piping networks. *Water (Switzerland)*, 9(10), 1–21.
- Laucelli, D., & Menconi, S. (2015). Water distribution network analysis accounting for different background leakage models. *Procedia Eng.* 119(1), 680–689.
- Ávila, C. A. M., Sánchez-Romero, F. J., López-Jiménez, P. A., & Pérez-Sánchez, M. (2021). Optimization tool to improve the management of the leakages and recovered energy in irrigation water systems. *Agric. Water Manag.*, 258, Article 107223. Dec.
- Rossman, L. A. (1999). The EPANET Programmer's Toolkit for Analysis of Water Distribution Systems. *WRPMD 1999 Prep. 21st Century*, 1–10.
- Moriasi, D. N., Arnold, J. G., Van Liew, M. W., Binger, R. L., Harmel, R. D., & Veith, T. L. (2007). Model evaluation guidelines for systematic quantification of accuracy in watershed simulations. *Trans. ASABE*, 50(3), 885–900.
- del Teso, R., Gómez, E., Estruch-Juan, E., & Cabrera, E. (2019). Topographic Energy Management in Water Distribution Systems. *Water Resour. Manag.*, 33(12), 4385–4400.
- Pérez-Sánchez, M., Sánchez-Romero, F. J., Ramos, H. M., & López-Jiménez, P. A. (2017). Optimization strategy for improving the energy efficiency of irrigation systems by micro hydropower: Practical application. *Water (Switzerland)*, 9(10).
- Rosado, L. E. C., López-Jiménez, P. A., Sánchez-Romero, F. J., Fuertes, P. C., & Pérez-Sánchez, M. (2020). Applied strategy to characterize the energy improvement using PATs in a water supply system. *Water (Switzerland)*, 12(6), 1–22.
- Pérez-Sánchez, M., Sánchez-Romero, F. J., López-Jiménez, P. A., & Ramos, H. M. (2018). PATs selection towards sustainability in irrigation networks: Simulated annealing as a water management tool. *Renew. Energy*, 116, 234–249.
- Pérez-Sánchez, M., Sánchez-Romero, F. J., Ramos, H. M., & López-Jiménez, P. A. (2020). Improved planning of energy recovery in water systems using a new analytic approach to PAT performance curves. *Water (Switzerland)*, 12(2).
- Macías Ávila, C. A., Sánchez-Romero, F. J., López-Jiménez, P. A., & Pérez-Sánchez, M. (2021). Definition of the operational curves by modification of the affinity laws to improve the simulation of pats. *Water (Switzerland)*, 13(14), 1–17.
- Renaud, E., Sissoko, M. T., Clauzier, M., Gilbert, D., & Khedhaouiria, D. (2012). Comparative study of different methods to assess average pressures in water distribution zones - Archive ouverte HAL. *waterloss*.
- Lugauer, F. J., Kainz, J., & Gaderer, M. (2021). Techno-Economic Efficiency Analysis of Various Operating Strategies for Micro-Hydro Storage Using a Pump as a Turbine. *Energies* 2021, 14(2), 425. Vol. 14, Page 425Jan.
- De Marchis, M., Milici, B., Volpe, R., & Messineo, A. (2016). Energy Saving in Water Distribution Network through Pump as Turbine Generators: Economic and Environmental Analysis. *Energies* 2016, 9(11), 877. Vol. 9, Page 877Oct.